Excluded-Volume Effects on the Mean-Square Radius of Gyration and Intrinsic Viscosity of Oligo- and Poly(methyl methacrylate)s

Fumiaki Abe, Ken Horita, Yoshiyuki Einaga, and Hiromi Yamakawa*

Department of Polymer Chemistry, Kyoto University, Kyoto 606-01, Japan

*Received September 29, 1993; Revised Manuscript Received November 10, 1993**

ABSTRACT: The mean-square radius of gyration $\langle S^2 \rangle$ and intrinsic viscosity $[\eta]$ were determined for atactic poly(methyl methacrylate) (a-PMMA) in acetone at 25.0 °C, in nitroethane at 30.0 °C, and in chloroform at 25.0 °C in the range of weight-average molecular weight M_w from 6.02×10^2 to 1.58×10^6. The present results for the gyration- and viscosity-radius expansion factors α_S and α_η for a-PMMA along with the previous ones for atactic polystyrene (a-PS) and polyisobutylene are found to become functions only of the scaled excluded-volume parameter $\tilde{z}$ defined in the Yamakawa–Stockmayer–Shimada (YSS) theory based on the helical wormlike chain model. Here, α_η for a-PMMA has been calculated by taking account of the dependence on solvent of the Flory–Fox factor Φ_∞ (or Φ_Θ defined in this paper). It is shown that $\alpha_S(\tilde{z})$ may be quantitatively explained by the YSS theory, while $\alpha_\eta(\tilde{z})$ may be approximately explained by the Barrett equation for α_η with $\tilde{z}$ in place of the conventional excluded-volume parameter z. Thus the present results confirm that the quasi-two-parameter scheme is valid for both α_S and α_η irrespective of the large differences in chain stiffness, local chain conformation, and solvent condition, indicating that there is no draining effect in α_η at least for the present systems. It is found that the effect of chain stiffness on α_S and α_η for a-PMMA remains large even for $M_w > 10^6$ as in the case of a-PS. The unperturbed values $\langle S^2 \rangle_0$ of $\langle S^2 \rangle$ for a-PMMA in acetone at 25.0 °C, in acetonitrile at 44.0 °C (Θ), and in *n*-butyl chloride at 40.8 °C (Θ) are found to coincide with each other, indicating that $\langle S^2 \rangle_0$ of a-PMMA is independent of solvent in contradiction to the prevailing view. Its dependence on solvent for a-PMMA that has been exclusively obtained so far from the Stockmayer–Fixman plot of $[\eta]$ is only apparent and the dependence on solvent of $[\eta]_\Theta$ must be regarded as arising from that of Φ_∞.

Introduction

In previous papers[1–3] of this series, we have shown that a *quasi*-two-parameter scheme is valid for the gyration- and viscosity-radius expansion factors α_S and α_η for atactic polystyrene (a-PS) and polyisobutylene (PIB). That is, both α_S and α_η for them may be expressed as functions only of the scaled excluded-volume parameter $\tilde{z}$ defined in the Yamakawa–Stockmayer–Shimada (YSS) theory[4–6] that takes account of the effects of excluded volume and chain stiffness on the basis of the helical wormlike (HW) chain,[7,8] including the Kratky–Porod wormlike chain[9] as its special case, over a wide range of molecular weight M including the oligomer region, irrespective of the difference in solvent condition. It has also been found that the effects of chain stiffness on α_S and α_η remain large for such large M that the ratio of the unperturbed mean-square radius of gyration $\langle S^2 \rangle_0$ to M already reaches its coil-limiting value independent of M. In the present study, we extend the work to atactic oligo- and poly(methyl methacrylate)s (a-PMMA) with the fraction of racemic diads $f_r = 0.79$.

We have already investigated extensively dilute solution properties of a-PMMA in the Θ state.[10–14] As for $\langle S^2 \rangle_0$ and the intrinsic viscosity $[\eta]_\Theta$, it has been found that the ratio of $\langle S^2 \rangle_0$ to the weight-average molecular weight M_w as a function of M_w exhibits a maximum before reaching its coil-limiting value[10] and that a double-logarithmic plot of $[\eta]_\Theta$ against M_w deviates appreciably upward from its asymptotic straight line of slope $^1/_2$ with decreasing M_w following an inverse S-shaped curve.[11] It has then been shown that all the findings characteristic of a-PMMA, including these results, may well be explained consistently on the basis of the HW chain model and that, in contradiction to the prevailing view, the a-PMMA chain has rather large stiffness, retaining its large helical portions in dilute solution, compared to other flexible polymers, e.g., a-PS and PIB. Thus the object of the present work is to examine whether the quasi-two-parameter scheme for α_S and α_η is valid also for a-PMMA in various solvents, which is remarkably different from a-PS and PIB in chain stiffness and local chain conformation.

In the previous studies of the excluded-volume effects,[1–3,15] we have given particular attention to correct determination of α_S and α_η by choosing properly a pair of good and Θ solvents so that the unperturbed values of the mean-square radius of gyration $\langle S^2 \rangle$ and the intrinsic viscosity $[\eta]$ in that good solvent may coincide with those in the Θ state taken as the reference standards. For this purpose, in practice by preliminary viscosity measurements, we have confirmed the coincidence between the values of $[\eta]$ of a-PS or PIB in the good and Θ solvents for each solvent pair in the oligomer region where the excluded-volume effect may be negligible.

For a-PMMA, however, the same procedure cannot be applied. It has been found[11,16] that the values of $[\eta]_\Theta/M_w^{1/2}$ of a-PMMA samples with sufficiently large M_w in two Θ solvents at their respective Θ temperatures, i.e., in acetonitrile at 44.0 °C and in *n*-butyl chloride at 40.8 °C, are definitely different from each other, although those of $\langle S^2 \rangle_0/M_w$ coincide within experimental error. It is then concluded that the coil-limiting values Φ_∞ of the Flory–Fox factor for the a-PMMA chain in the two Θ solvents are different from each other. This indicates that the values of $[\eta]$ for a-PMMA oligomer samples cannot be used to estimate their unperturbed dimension, in contrast to the cases of a-PS and PIB. (In this connection, we note that Φ_∞ of a-PS in the Θ state has been found to be independent of solvent as far as *trans*-decalin and cyclohexane are concerned, while the dependence of Φ_∞ on solvent has not been investigated for PIB.) Thus, in this work, we confirm directly that the values of $\langle S^2 \rangle$ of a-PMMA in acetone at 25.0 °C chosen as a typical good solvent for it agree with those in acetonitrile at Θ in the oligomer region. As discussed below, the dependence of

* Abstract published in *Advance ACS Abstracts*, January 1, 1994.

0024-9297/94/2227-0725$04.50/0

Table 1. Values of M_w, x_w, and M_w/M_n for Atactic Oligo- and Poly(methyl methacrylate)s

sample	M_w	x_w	M_w/M_n
OM6[a]	6.02×10^2	6.00	1.00
OM12	1.16×10^3	11.6	1.02
OM18[b]	1.80×10^3	18.0	1.07
OM22	2.23×10^3	22.3	1.06
OM42	4.18×10^3	41.8	1.09
OM76	7.55×10^3	75.5	1.08
MM1[c]	1.09×10^4	109	1.06
MM2a	2.02×10^4	202	1.08
MM4	3.53×10^4	353	1.07
MM5	5.16×10^4	516	1.07
MM7	7.40×10^4	740	1.09
MM12	1.19×10^5	1190	1.09
MM20	2.04×10^5	2040	1.08
MM31	3.12×10^5	3120	1.08
Mr5	4.82×10^5	4820	1.07
Mr8a	7.65×10^5	7650	1.07
Mr16	1.58×10^6	15800	1.08

[a] M_w of OM6 had been determined by analytical GPC.[10] [b] M_w's of OM18 and OM22 had been determined from LS measurements in acetone at 25.0 °C.[10] [c] M_w's of MM1 and MM4 through MM12 had been determined from LS measurements in acetonitrile at 44.0 °C.[10]

Φ_∞ on solvent also causes a difficulty in the determination of α_η for a-PMMA.

Experimental Section

Materials. Most of the a-PMMA samples used in this work are the same as those used in the previous studies,[10-14] i.e., the fractions separated by preparative gel permeation chromatography (GPC) or fractional precipitation from the original samples prepared by group-transfer polymerization (GTP). For this and previous studies,[14] some additional samples were prepared in the same manner as before,[10] i.e., by GTP and also by radical polymerization, followed by separation by preparative GPC or by fractional precipitation. The values of f_r for them were examined by ^{13}C NMR in the same manner as before[10] and were found to coincide with the previous value 0.79 independent of M_w.

The values of M_w determined from light scattering (LS) measurements for the samples with $M_w > 10^3$ and by analytical GPC for the sample OM6 are given in Table 1 along with those of the weight-average degree of polymerization x_w and the ratio of M_w to the number-average molecular weight M_n. The samples OM12, OM42, OM76, MM2a, and MM20 through Mr16 are the additional ones, and their M_w's were determined from LS measurements in acetone at 25.0 °C. (The results for the first four of them have already been reported elsewhere.[14]) The values of M_w/M_n indicate that the molecular weight distributions of all the samples are sufficiently narrow for the present purpose.

The solvents acetonitrile, acetone, nitroethane, and chloroform used for LS and viscosity measurements were purified according to standard procedures.

Light Scattering. LS measurements were carried out to determine $\langle S^2 \rangle$ (and also M_w) of five samples with $M_w \gtrsim 2.0 \times 10^5$ in acetone at 25.0 °C, in nitroethane at 30.0 °C, and in chloroform at 25.0 °C and of three samples with $M_w \gtrsim 5.0 \times 10^5$ in acetonitrile at 44.0 °C (Θ). Measurements were also made for the samples OM12, OM42, OM76, and MM2a in acetone at 25.0 °C to determine their M_w's. A Fica 50 light-scattering photometer was used for all the measurements with vertically polarized incident light of wavelength 436 nm. For a calibration of the apparatus, the intensity of light scattered from pure benzene was measured at 25.0 °C at a scattering angle of 90°, where the Rayleigh ratio $R_{Uu}(90°)$ of pure benzene was taken as 46.5×10^{-6} cm^{-1}. The depolarization ratio ρ_u of pure benzene at 25.0 °C was found to be 0.41 ± 0.01. Scattering intensities were measured at 5–8 different concentrations and at scattering angles ranging from 30 to 150°, except for Mr16 in the three good solvents and for Mr8a in chloroform. For the latter cases, the intensities were measured at 10–12 scattering angles ranging from 22.5 to 60° or from 30 to 75° for Mr16 in the good solvents and from 30 to 120° for Mr8a in chloroform. The correction for anisotropic scattering was applied to the solutions of the sample OM12 in acetone according to the procedure described previously.[17] All the data obtained were analyzed by the Berry square-root plot.[18]

The most concentrated solutions of each sample were prepared by continuous stirring at room temperature for ca. 1 day in the three good solvents, preventing them from being exposed to light in the cases of nitroethane and chloroform solutions, and at ca. 50 °C for 4 days in acetonitrile. They were optically purified by filtration through a Teflon membrane of pore size 0.45 or 0.10 μm. The solutions of lower concentrations were obtained by successive dilution. The polymer mass concentrations c were calculated from the weight fractions with the densities of the solutions. The densities of the solvents and solutions were measured with a pycnometer of the Lipkin–Davison type.

The values of the refractive index increment $\partial n/\partial c$ measured with a Shimadzu differential refractometer at 436 nm were 0.097_5 and 0.063_0 cm^3/g for a-PMMA with $M_w \gtrsim 2.0 \times 10^5$ in nitroethane at 30.0 °C and in chloroform at 25.0 °C, respectively. For the values of $\partial n/\partial c$ at 436 nm for a-PMMA in the other solvents, the results reported previously[10] were used. The values of $\partial n/\partial c$ for the oligomer samples in acetone at 25.0 °C are given in the Appendix.

Small-Angle X-ray Scattering. Small-angle X-ray scattering (SAXS) measurements were carried out for seven a-PMMA samples with $M_w \lesssim 5.0 \times 10^4$ in acetone at 25.0 °C by the use of an Anton Paar Kratky U-slit camera with an incident X-ray of wavelength 1.54 Å (Cu Kα line). The apparatus system and the method of data acquisition and analysis are the same as those described in the previous paper.[19]

The measurements were performed for four to seven solutions of different concentrations for each polymer sample and for the solvent at scattering angles ranging from 1×10^{-3} rad to a value at which the scattering intensity was negligibly small. Corrections for the stability of the X-ray source and the detector electronics were made by measuring the intensity scattered from Lupolene (a platelet of polyethylene) used as a working standard before and after each measurement of a given sample solution and the solvent. The effect of absorption of X-ray by a given solution or solvent was also corrected by measuring the intensity scattered from Lupolene with insertion of the solution or solvent between the X-ray source and Lupolene. The degree of absorption increased linearly with increasing solute concentration.

The excess reduced scattering intensities were obtained from the observed (smeared) excess reduced intensities by the modified Glatter desmearing method, which consists of expressing the true scattering function in terms of cubic B-spline functions, as described previously.[19] All the data were processed by the use of a Fujitsu M-1800/30 digital computer in this university. Then the desmeared excess reduced intensities were analyzed by the Berry square-root plot as in the case of LS measurements to determine the apparent mean-square radius of gyration $\langle S^2 \rangle_s$. Then $\langle S^2 \rangle$ (of the chain contour) was obtained from $\langle S^2 \rangle_s$ as before by the use of the equation

$$\langle S^2 \rangle_s = \langle S^2 \rangle + S_c^2 \quad (1)$$

which was derived for a continuous chain having a uniform circular cross section, with S_c being the radius of gyration of the cross section.[19] In this work, we make the above correction by adopting the value 8.4 Å^2 of S_c^2 estimated from the data for the partial specific volume v_2 of a-PMMA in acetonitrile at 44.0 °C, as done previously.[10] We note that the value of v_2 of a-PMMA in acetone at 25.0 °C is approximately equal to that in acetonitrile at 44.0 °C for sufficiently large M_w.

The solutions of each sample were prepared in the same manner as in the case of LS measurements.

Viscosity. Viscosity measurements were carried out for almost all the samples in acetone at 25.0 °C, in nitroethane at 30.0 °C, and in chloroform at 25.0 °C and also for several samples in acetonitrile at 44.0 °C (Θ). We used conventional capillary and four-bulb spiral capillary viscometers of the Ubbelohde type. In all the measurements, the flow time was measured to a precision of 0.1 s, keeping the difference between flow times of the solvent and solution larger than ca. 20 s. The test solutions were maintained at constant temperature within ±0.005 °C during the measurements. The data obtained were treated as usual by

Table 2. Results of LS and SAXS Measurements on Atactic Oligo- and Poly(methyl methacrylate)s in Acetonitrile at 44.0 °C (Θ) and in Good Solvents

	acetonitrile (44.0 °C)		acetone (25.0 °C)		nitroethane (30.0 °C)		chloroform (25.0 °C)	
sample	$10^{-4}M_w$	$\langle S^2\rangle_0^{1/2}$, Å	$10^{-4}M_w$	$\langle S^2\rangle^{1/2}$, Å	$10^{-4}M_w$	$\langle S^2\rangle^{1/2}$, Å	$10^{-4}M_w$	$\langle S^2\rangle^{1/2}$, Å
OM6[a]		4.30		4.39				
OM18		10.9	0.180	11.1				
OM42			0.418	17.1				
OM76			0.755	23.1				
MM2a			2.02	38.3				
MM4	3.53	48.0	3.40	53.2				
MM5	5.16	56.4	5.04	64.0				
MM20			20.4	140	19.8	159	20.5	183
MM31			31.2	179	30.6	201	31.1	237
Mr5	49.8	179	48.2	232	47.9	266	48.6	305
Mr8a	79.0	224	76.5	301	76.3	348	77.8	405
Mr16	157	321	158	464	155	546	161	641

[a] The data for OM6, OM18, MM4, and MM5 in acetonitrile at 44.0 °C and for M_w of OM18 and MM5 in acetone at 25.0 °C have been reproduced from ref 10. The values of $\langle S^2\rangle_0^{1/2}$ and $\langle S^2\rangle^{1/2}$ smaller than 100 Å have been determined from SAXS measurements.

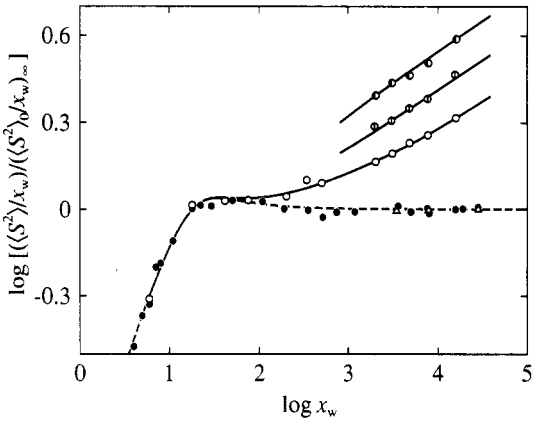

Figure 1. Double-logarithmic plots of $(\langle S^2\rangle/x_w)/(\langle S^2\rangle_0/x_w)_\infty$ against x_w for the a-PMMA samples with $f_r = 0.79$: (○) in acetone at 25.0 °C; (◑) in nitroethane at 30.0 °C; (◐) in chloroform at 25.0 °C; (●) in acetonitrile at 44.0 °C (Θ) (reproduced from ref 10, except for the samples Mr5, Mr8a, and Mr16); (△) in *n*-butyl chloride at 40.8 °C (Θ) (reproduced from ref 11). For acetonitrile and *n*-butyl chloride solutions, $\langle S^2\rangle/x_w$ refers to $\langle S^2\rangle_0/x_w$. The solid curves connect the data points smoothly, while the dashed curve represents the HW theoretical values (see the text).

the Huggins and Fuoss–Mead plots to determine $[\eta]$ and the Huggins coefficient k'.

The test solutions were prepared in the same manner as in the case of LS measurements. Density corrections were made in the calculation of c and also of the relative viscosity from the flow times of the solution and solvent.

Results

Mean-Square Radius of Gyration. The values of $\langle S^2\rangle^{1/2}$ obtained from LS and SAXS measurements are listed in Table 2 along with those of M_w determined from LS measurements. It also includes the results for $\langle S^2\rangle_0^{1/2}$ and M_w obtained previously[10] for the same samples. Figure 1 shows double-logarithmic plots of the ratio $(\langle S^2\rangle/x_w)/(\langle S^2\rangle_0/x_w)_\infty$ against x_w for the present results for a-PMMA in acetonitrile at 44.0 °C (Θ) (filled circles), in acetone at 25.0 °C (unfilled circles), in nitroethane at 30.0 °C (circles with vertical bar), and in chloroform at 25.0 °C (half-filled circles), along with those obtained previously in acetonitrile at Θ (filled circles)[10] and in *n*-butyl chloride at 40.8 °C (Θ) (triangles).[11] Here, $(\langle S^2\rangle_0/x_w)_\infty$ denotes the value of the ratio $\langle S^2\rangle_0/x_w$ for the infinitely long unperturbed chain and has been taken as 6.57 Å^2 from the LS data for the seven highest-molecular-weight samples in acetonitrile at Θ. The solid curves connect the data points smoothly, while the dashed curve represents the best-fit HW theoretical values calculated with the model parameters determined previously.[10] (The values of the HW model parameters are listed in Table 5.)

As already reported[11,16] and also described above, the values of $\langle S^2\rangle_0$ in the two Θ solvents, acetonitrile and *n*-butyl chloride, coincide with each other within experimental error. It is seen that the values of $\langle S^2\rangle$ in acetone at 25.0 °C agree with those in acetonitrile at Θ in the oligomer region for $M_w \lesssim 4 \times 10^3$. Thus we may conclude that the dependence on solvent of the unperturbed dimension of the a-PMMA chain is negligible, in contradiction to the prevailing view,[20,21] as far as these solvents are concerned. The present findings for a-PMMA are in marked contrast to the case of a-PS, for which the values of $\langle S^2\rangle_0$ in two Θ solvents, i.e., cyclohexane at 34.5 °C and *trans*-decalin at 21.0 °C, are definitely different from each other.[3,16] The results for the acetone solutions assure that α_S of a-PMMA in this solvent can be correctly calculated by taking the values of $\langle S^2\rangle_0$ in acetonitrile at Θ as the reference standards. In the present work, we also calculate α_S of a-PMMA in nitroethane at 30.0 °C and in chloroform at 25.0 °C by the use of the values of $\langle S^2\rangle_0$ in acetonitrile at Θ, assuming that the dependence of $\langle S^2\rangle_0$ on solvent is negligible.

As seen from Figure 1, the excluded-volume effect on $\langle S^2\rangle$ of a-PMMA in acetone becomes appreciable for $x_w \gtrsim 40$. We note that this critical value of x_w for the onset of the effect corresponds to the value ca. 1.9 of the reduced contour length, which is close to the corresponding value ca. 2.1 for a-PS.[1]

Intrinsic Viscosity. The values of $[\eta]$ determined for all the samples in acetonitrile at 44.0 °C (Θ), in acetone at 25.0 °C, in nitroethane at 30.0 °C, and in chloroform at 25.0 °C are summarized in Table 3 along with those of k'. It also includes the results obtained previously[11] for the same samples in acetonitrile at Θ. Figure 2 shows double-logarithmic plots of the ratio $[\eta]/M_w^{1/2}$ against M_w for the results in acetonitrile (filled circles), in acetone (unfilled circles), in nitroethane (circles with vertical bar), and in chloroform (half-filled circles). The previous data for the same a-PMMA samples in acetonitrile (filled circles) and in *n*-butyl chloride (filled triangles) at Θ have been reproduced from ref 11, for reference. The solid and dashed curves connect the data points smoothly (the latter for the *n*-butyl chloride solutions).

As previously mentioned,[11] the values of $[\eta]_\Theta$ in *n*-butyl chloride at Θ are clearly larger than those in acetonitrile at Θ over the whole range of M_w studied, despite the fact that those of $\langle S^2\rangle_0$ in the two Θ solvents coincide with each other. This leads to the difference between the Flory–Fox factors for the a-PMMA chain in these solvents.[16]

Table 3. Results of Viscometry on Atactic Oligo- and Poly(methyl methacrylate)s in Acetonitrile at 44.0 °C (Θ) and in Good Solvents

	acetonitrile (44.0 °C)		acetone (25.0 °C)		nitroethane (30.0 °C)		chloroform (25.0 °C)	
sample	$[\eta]_\Theta$, dL/g	k'	$[\eta]$, dL/g	k'	$[\eta]$, dL/g	k'	$[\eta]$, dL/g	k'
OM12			0.0330	0.90				
OM18[a]	0.0357	0.93	0.0392	1.1				
OM22	0.0390	0.93			0.0392	1.1	0.0508	0.62
OM42			0.0524	0.88	0.0515	0.74		
OM76	0.0570	0.95	0.0653	1.0	0.0690	0.66	0.0910	0.61
MM1	0.0673	1.0	0.0749	0.70				
MM2a	0.0826	1.0	0.101	0.80	0.122	0.52	0.166	0.47
MM4	0.106	1.1	0.139	0.74	0.162	0.49	0.235	0.45
MM5	0.124	0.90	0.166	0.72	0.212	0.45	0.312	0.41
MM7	0.150	1.0	0.214	0.65	0.278	0.43	0.421	0.38
MM12	0.194	1.1	0.287	0.58	0.385	0.41	0.588	0.39
MM20	0.247	1.0	0.409	0.68	0.564	0.36	0.884	0.38
MM31	0.305	0.98	0.542	0.56	0.757	0.35	1.20	0.37
Mr5	0.385	1.0	0.723	0.52	1.06	0.36	1.71	0.34
Mr8a	0.486	1.2	0.997	0.52	1.48	0.36	2.42	0.34
Mr16	0.719	1.1	1.69	0.42	2.55	0.35	4.28	0.35

[a] The data for OM18 through MM12 in acetonitrile at 44.0 °C (Θ) have been reproduced from ref 11, except for OM76 and MM2a (present work).

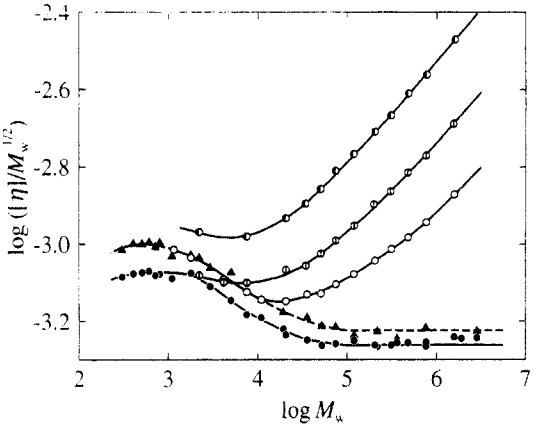

Figure 2. Double-logarithmic plots of $[\eta]/M_w^{1/2}$ ($[\eta]$ in dL/g) against M_w for a-PMMA: (▲) in *n*-butyl chloride at 40.8 °C (Θ) (reproduced from ref 11). The other symbols have the same meaning as those in Figure 1. The solid and dashed curves connect the data points smoothly (the latter for the *n*-butyl chloride solutions).

In the oligomer region, the values of $[\eta]$ in acetone are in agreement with those in *n*-butyl chloride at Θ but definitely larger than those in acetonitrile at Θ, although the values of $\langle S^2\rangle$ in acetone agree with those in the latter Θ solvent as shown in Figure 1. It is also seen from Figure 2 that $[\eta]$ of the oligomer sample OM22 in chloroform has a significantly larger value than those in the two Θ solvents. Thus, if we calculate α_η for the a-PMMA chain in the three good solvents by the use of the values of $[\eta]_\Theta$ in acetonitrile at Θ in accordance with the calculation of α_S, then such α_η, which we designate by $\bar{\alpha}_\eta$, has only the meaning of an *apparent* viscosity-radius expansion factor, as discussed below.

Discussion

Comparison of the Results for α_S with the YSS Theory. We first analyze the results for α_S on the basis of the YSS theory.[4-6] The values of α_S^2 calculated from

$$\langle S^2\rangle = \langle S^2\rangle_0 \alpha_S^{\,2} \tag{2}$$

with the values of $\langle S^2\rangle^{1/2}$ and $\langle S^2\rangle_0^{1/2}$ given in Table 2 are summarized in Table 4, where for the samples OM42, OM76, MM2a, MM20, and MM31 in acetone at 25.0 °C we have used the values of $\langle S^2\rangle_0^{1/2}$ obtained by interpolation from those for the same a-PMMA samples determined in the present and previous studies (Tables III and IV of ref 10).

Table 4. Values of α_S^2 and $\bar{\alpha}_\eta^3$ of Oligo- and Poly(methyl methacrylate)s in Good Solvents

	acetone (25.0 °C)		nitroethane (30.0 °C)		chloroform (25.0 °C)	
sample	α_S^2	$\bar{\alpha}_\eta^3$	α_S^2	$\bar{\alpha}_\eta^3$	α_S^2	$\bar{\alpha}_\eta^3$
OM6	1.04					
OM18	1.04					
OM42	1.00					
OM76	1.04	1.15		1.21		1.60
MM1		1.11				
MM2a	1.10	1.22		1.48		2.01
MM4	1.23	1.31		1.53		2.22
MM5	1.29	1.34		1.71		2.52
MM7		1.43		1.85		2.81
MM12		1.48		1.98		3.03
MM20	1.47	1.66	1.96	2.28	2.50	3.58
MM31	1.57	1.78	2.02	2.48	2.77	3.93
Mr5	1.68	1.88	2.21	2.75	2.90	4.44
Mr8a	1.81	2.05	2.41	3.05	3.27	4.98
Mr16	2.09	2.35	2.89	3.55	3.99	5.95

Now we reproduce necessary basic equations, for convenience. For the HW chain of total contour length L, the YSS theory assumes the Domb–Barrett expression[22] for α_S^2, i.e.,

$$\alpha_S^{\,2} = [1 + 10\tilde{z} + (70\pi/9 + 10/3)\tilde{z}^2 + 8\pi^{3/2}\tilde{z}^3]^{2/15}[0.933 + 0.067\exp(-0.85\tilde{z} - 1.39\tilde{z}^2)] \tag{3}$$

with the scaled excluded-volume parameter $\tilde{z}$ defined by

$$\tilde{z} = (3/4)K(\lambda L)z \tag{4}$$

in place of the conventional excluded-volume parameter z. The latter is now defined by

$$z = (3/2\pi)^{3/2}(\lambda B)(\lambda L)^{1/2} \tag{5}$$

where

$$B = \beta/a^2 c_\infty^{\,3/2} \tag{6}$$

with

$$c_\infty = \lim_{\lambda L\to\infty}(6\lambda\langle S^2\rangle_0/L) = \frac{4 + (\lambda^{-1}\tau_0)^2}{4 + (\lambda^{-1}\kappa_0)^2 + (\lambda^{-1}\tau_0)^2} \tag{7}$$

Here, λ^{-1} is the static stiffness parameter of the HW chain, κ_0 and τ_0 are the differential-geometrical curvature and torsion, respectively, of its characteristic helix taken at the minimum zero of its elastic energy, β is the binary-cluster integral between beads with a their spacing. In eq 4, the coefficient $K(L)$ is given by

$$K(L) = \frac{4}{3} - 2.711L^{-1/2} + \frac{7}{6}L^{-1} \quad \text{for } L > 6$$
$$= L^{-1/2}\exp(-6.611L^{-1} + 0.9198 + 0.03516L) \quad \text{for } L \le 6 \tag{8}$$

Note that L is related to the degree of polymerization x by the equation

$$L = xM_0/M_L \tag{9}$$

where M_0 is the molecular weight of the repeat unit of a given real chain and M_L is the shift factor as defined as the molecular weight per unit contour length.

Table 5. Values of the HW Model Parameters and the Reduced Parameter λB for Atactic Poly(methyl methacrylate)

solvent	temp, °C	$\lambda^{-1}\kappa_0$	$\lambda^{-1}\tau_0$	λ^{-1}, Å	M_L, Å^{-1}	λB
acetonitrile[a]	44.0	4.0	1.1	57.9	36.3	0
acetone	25.0					0.22
nitroethane	30.0					0.52
chloroform	25.0					1.15

[a] Reproduced from ref 10.

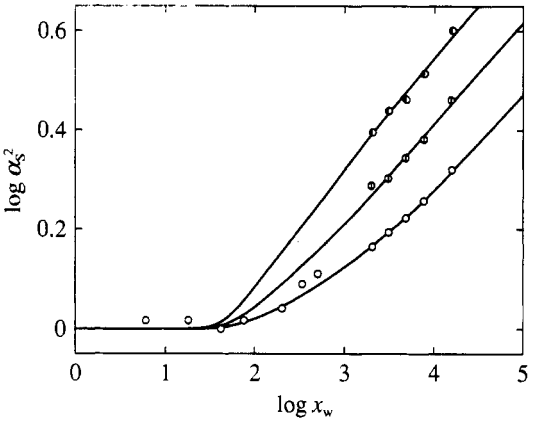

Figure 3. Double-logarithmic plots of α_S^2 against x_w for a-PMMA in acetone at 25.0 °C, in nitroethane at 30.0 °C, and in chloroform at 25.0 °C. The symbols have the same meaning as those in Figure 1. The solid curves represent the best-fit YSS theory values (see the text).

For a comparison between the experimental and theoretical values of α_S, we need the values of the HW model parameters $\lambda^{-1}\kappa_0$, $\lambda^{-1}\tau_0$, λ^{-1}, and M_L and the reduced excluded-volume strength λB. The values of the HW model parameters for a-PMMA have already been determined from a comparison between the HW theory[7,8] and the experimental results for $\langle S^2\rangle_0$ in acetonitrile at θ,[10] as reproduced in the first row of Table 5. We may adopt these parameter values for the a-PMMA chain in the three good solvents used in this study, according to the solvent independence of $\langle S^2\rangle_0$ mentioned above. The remaining parameter λB may be determined from a comparison of experimental data for α_S with the YSS theory, as done previously.[1-3]

Figure 3 shows double-logarithmic plots of α_S^2 against x_w for a-PMMA in the three solvents, acetone (unfilled circles), nitroethane (circles with vertical bar), and chloroform (half-filled circles). The solid curves represent the best-fit YSS theory values calculated from eq 3 with eqs 4, 5, 8, and 9. The results for λB thus determined from the curve fitting are given in the seventh column of Table 5. It is seen that the YSS theory may explain quantitatively the x_w dependence of α_S for all solvent systems, and, in particular, there is good agreement between theory and experiment over the whole range of x_w studied for the acetone solutions. The critical value of x_w for the onset of the excluded-volume effect is seen to be almost independent of solvent quality. It is rather surprising to find that the curve fitted to the data for the chloroform solutions is convex upward for $x_w \gtrsim 500$. We note that the Chen–Noolandi theory,[23] which also takes account of the effect of chain stiffness on α_S, does not agree with the experimental results for a-PMMA as well as for a-PS (see Figure 7 of ref 1), although the comparison is not explicitly shown.

The same data for α_S^2 as in Figure 3 are double-logarithmically plotted against z in Figure 4, where the values of z have been calculated from eq 5 with eq 9 with the values of the parameters given in Table 5. The solid curves represent the YSS theory values. For comparison,

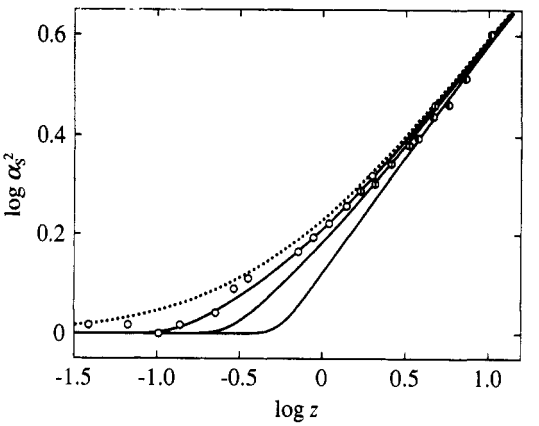

Figure 4. Double-logarithmic plots of α_S^2 against z for a-PMMA in acetone at 25.0 °C, in nitroethane at 30.0 °C, and in chloroform at 25.0 °C. The symbols have the same meaning as those in Figure 1. The solid curves represent the best-fit YSS theory values, and the dotted curve represents the conventional two-parameter theory values (see the text).

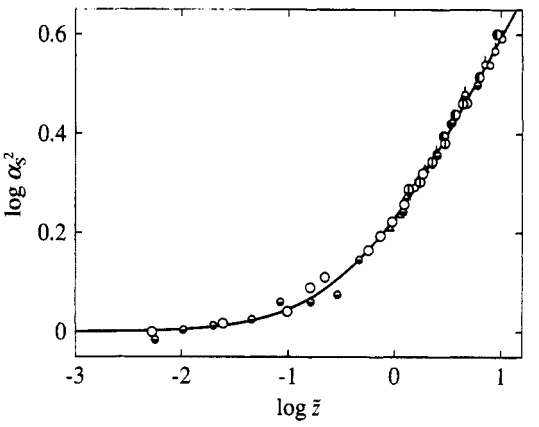

Figure 5. Double-logarithmic plots of α_S^2 against $\tilde{z}$ for a-PMMA, a-PS, and PIB: (○) a-PMMA in acetone at 25.0 °C; (◑) a-PMMA in nitroethane at 30.0 °C; (◐) a-PMMA in chloroform at 25.0 °C; (⊖) a-PS in toluene at 15.0 °C;[1] (⌀, ◊) a-PS in benzene at 25.0 °C;[3] (△) PIB in *n*-heptane at 25.0 °C.[2] The solid curve represents the YSS theory values (see the text).

the two-parameter-theory values calculated from eq 3 with the values of λB in Table 5 but with $K = {}^4/_3$ (the coil-limiting value) are shown by the dotted curve. The solid curves do not form a single composite curve but deviate downward progressively from the dotted curve with decreasing z (or decreasing L) because of the effect of chain stiffness. This effect becomes more significant as λB is increased or, in other words, as the solvent quality becomes better. The effect on α_S remains rather large even at large $z \simeq 10$ or at very large $M_w \gtrsim 10^6$, as in the case of a-PS.[1]

Figure 5 shows double-logarithmic plots of α_S^2 against $\tilde{z}$ for the same data (large circles) as in Figures 3 and 4. The values of $\tilde{z}$ have been calculated from eq 4 with eq 8 and with the above values of z. The figure also includes the previous data for a-PS in toluene at 15.0 °C (small bottom-half-filled circles),[1] in benzene at 25.0 °C (small unfilled circles),[3] and for PIB in *n*-heptane at 25.0 °C (triangles).[2] The solid curve represents the YSS theory values calculated from eq 3. Although it is natural from the procedure of determining λB that all the data points form a single composite curve and are fitted by the solid curve, there is excellent agreement between theory and experiment over the whole range of $\tilde{z}$ or M_w studied irrespective of the differences in polymer species and solvent condition. The results imply that α_S is a function

only of $\tilde{z}$, the quasi-two-parameter scheme for it being valid for a-PMMA as well as for a-PS and PIB.

Relation between $\bar{\alpha}_\eta^3$ and α_S^3. As mentioned above, the dependence of the Flory–Fox factor Φ on solvent at Θ requires some consideration in the determination of α_η for a-PMMA. It is then convenient to express the intrinsic viscosities $[\eta]_\Theta$ in a given Θ solvent at Θ and $[\eta]$ in a given good solvent as

$$[\eta]_\Theta = 6^{3/2}\Phi_\Theta \frac{\langle S^2\rangle_\Theta^{3/2}}{M} \tag{10}$$

and

$$[\eta] = 6^{3/2}\Phi \frac{\langle S^2\rangle_0^{3/2}}{M}\alpha_S^3 \tag{11}$$

respectively, where Φ_Θ and $\langle S^2\rangle_\Theta$ are the values of Φ and $\langle S^2\rangle$ in that Θ solvent at Θ, respectively, and $\langle S^2\rangle_0$ is the unperturbed value of $\langle S^2\rangle$ in that good solvent. For a-PMMA, the relation $\langle S^2\rangle_0 = \langle S^2\rangle_\Theta$ may be considered to hold for any good and Θ solvent pair, as mentioned above.

Now if we define the cubed apparent viscosity-radius expansion factor $\bar{\alpha}_\eta^3$ by the equation

$$[\eta] = [\eta]_\Theta \bar{\alpha}_\eta^3 \tag{12}$$

following the conventional procedure of determining the viscosity-radius expansion factor, then $\bar{\alpha}_\eta^3$ may be written as

$$\bar{\alpha}_\eta^3 = (\Phi/\Phi_\Theta)\alpha_S^3 \tag{13}$$

Further, we define α_Φ by the equation

$$\Phi = \Phi_0\alpha_\Phi \tag{14}$$

with Φ_0 being the unperturbed value of Φ in the good solvent. Equation 13 may then be rewritten as

$$\bar{\alpha}_\eta^3 = C_\eta\alpha_\Phi\alpha_S^3 \tag{15}$$

with

$$C_\eta = \Phi_0/\Phi_\Theta \tag{16}$$

This C_η is essentially identical with the constant prefactor that has been previously[11] introduced to represent the dependence of Φ_Θ (or Φ_∞) on solvent. Thus the *true* viscosity-radius expansion factor α_η must be given by

$$\alpha_\eta^3 = \alpha_\Phi\alpha_S^3 = C\eta^{-1}\bar{\alpha}_\eta^3 \tag{17}$$

In the quasi-two-parameter scheme, both α_S and α_Φ must be functions only of $\tilde{z}$.

Values of $\bar{\alpha}_\eta^3$ calculated from eq 12 for a-PMMA in the three solvents with the values of $[\eta]$ and $[\eta]_\Theta$ given in Table 3 are summarized in Table 4. The results here require a comment. As seen from Figure 2, the dependence on M_w of $[\eta]/M_w^{1/2}$ of a-PMMA varies depending on solvent in the oligomer region. This implies that the bead friction (in the language of the HW touched bead model) also depends on solvent. Thus we have limited the calculation of $\bar{\alpha}_\eta^3$ to the range of $M_w \geq 7.55 \times 10^3$, although the range in which this effect exists is not known.

Figure 6 shows double-logarithmic plots of $\bar{\alpha}_\eta^3$ against α_S^3 for the present results for a-PMMA in the three solvents (large circles). It also includes the previous results for a-PS in toluene at 15.0 °C (small bottom-half-filled circles),[2] in benzene at 25.0 °C (small unfilled circles),[3] and in cyclohexane at 36.0–55.0 °C (small filled circles).[2] The solid and dashed curves connect the data points for

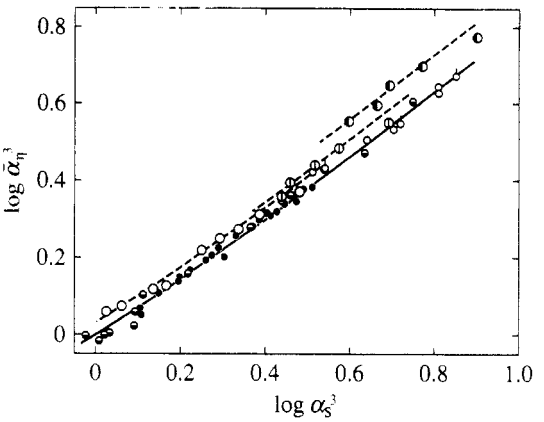

Figure 6. Double-logarithmic plots of $\bar{\alpha}_\eta^3$ against α_S^3 for a-PMMA and a-PS: (●) a-PS ($M_w > 10^7$) in cyclohexane at various temperatures (36.0–55.0 °C).[2] The other symbols have the same meaning as those in Figure 5. The solid and dashed curves connect the data points smoothly (see the text).

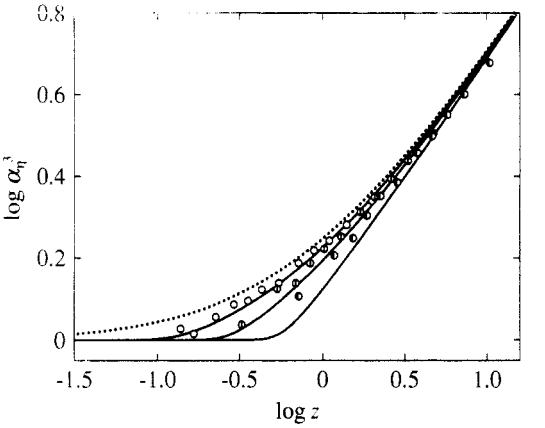

Figure 7. Double-logarithmic plots of α_η^3 against z for a-PMMA. The symbols have the same meaning as those in Figure 1. The solid curves represent the values calculated from eq 18, and the dotted curve represents the corresponding two-parameter-theory values (see the text).

a-PS and a-PMMA, respectively. It is seen that the data points (dashed curve) for a-PMMA in each solvent deviate upward from those (solid curve) for a-PS by a certain constant independent of α_S^3. (Note that α_S^3 for these data points have been correctly evaluated as described above.) It is seen from eq 15 that this constant may be equated to log C_η. The values of C_η thus estimated from the separations between the solid and dashed curves are 1.08, 1.11, and 1.25 for the acetone, nitroethane, and chloroform solutions, respectively. We note that $C_\eta = 1$ for a-PS since Φ (or Φ_∞) for a-PS is independent of solvent (as far as *trans*-decalin and cyclohexane are concerned) as stated above.

α_η^3 as a Function of z. The values of α_η^3 calculated from the second equality of eq 17 with those of $\bar{\alpha}_\eta^3$ in Table 4 and the above values of C_η for a-PMMA are double-logarithmically plotted against z in Figure 7, where we have calculated the values of z from eq 5 with eq 9 with the values of the HW model parameters determined from $\langle S^2\rangle_0$ and those of λB in Table 5. We note that the corresponding values of z for a-PS and PIB have been previously[2,3] calculated with the HW model parameters obtained from $[\eta]_\Theta$ and that the model parameters from $[\eta]_\Theta$ are less accurate than those from $\langle S^2\rangle_0$, especially for a-PMMA.

In the YSS scheme, we may also replace z by $\tilde{z}$ in any closed expression for α_η derived as a function of z. If we

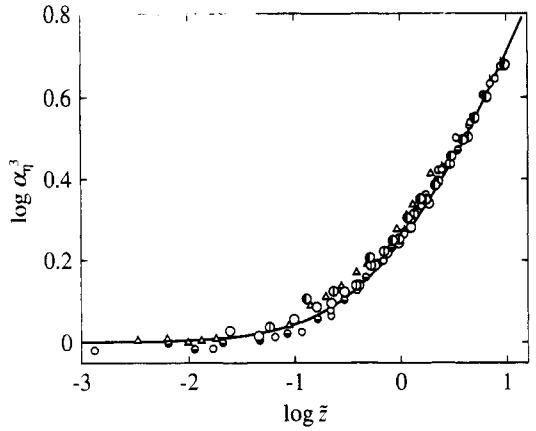

Figure 8. Double-logarithmic plots of α_η^3 against $\tilde{z}$ for a-PMMA, a-PS, and PIB. The symbols have the same meaning as those in Figure 5. The solid curve represents the values calculated from eq 18.

adopt the Barrett equation[24] as such an expression, we have

$$\alpha_\eta^3 = (1 + 3.8\tilde{z} + 1.9\tilde{z}^2)^{0.3} \quad (18)$$

In Figure 7, the solid curves represent the values of α_η^3 calculated from eq 18 with eqs 4, 5, 8, and 9 and with the values of the parameters given in Table 5. The dotted curve represents the two-parameter-theory values calculated similarly from eq 18 with $\tilde{z} = z$.

It is seen that the solid curves agree almost quantitatively with the data points for the acetone solutions (unfilled circles) over the whole range of z studied and with those for the nitroethane (circles with vertical bar) and chloroform (half-filled circles) solutions in the range of $z \gtrsim 2.5$. However, the theoretical values for the latter two deviate downward from the corresponding experimental values for $z \lesssim 2.5$. The discrepancy may be in part due to an overestimation of experimental α_η^3 resulting from the solvent dependence of the bead friction mentioned above (see also Figure 8). However, its main cause may be the incorrectness of the original Barrett equation. Note that it has been derived by combining a numerical solution of the Kirkwood–Riseman integral equation[25] for large z and the first-order perturbation equation by Shimada and Yamakawa.[26] The present results suggest that eq 18 may be too simple to apply over the whole range of z.

It is also seen that the data points deviate from the dotted curve more significantly with decreasing z (or M_w) and also with increasing λB (the excluded-volume strength) because of the effect of chain stiffness as in the case of α_S, which remains appreciable even for $z > 10$ or $M_w > 10^6$.

α_η^3 as a Function of $\tilde{z}$. Figure 8 shows double-logarithmic plots of α_η^3 against $\tilde{z}$ for the same data as in Figure 7 (large circles). It also includes the previous results for a-PS in toluene at 15.0 °C (small bottom-half-filled circles)[2] and in benzene at 25.0 °C (small unfilled circles)[3] and for PIB in n-heptane at 25.0 °C (small triangles),[2] for reference. The values of $\tilde{z}$ for a-PMMA have been calculated from eq 4 with eq 8 with those of z used in Figure 7, and correspondingly, those for a-PS and PIB have been recalculated by the use of the values of the HW model parameters determined from the respective data for $\langle S^2\rangle_0$. Thus the present plots for the latter two polymers are somewhat different from the previous ones, i.e., those in Figure 6 of ref 2 and in Figure 6 of ref 3. The solid curve represents the theoretical values calculated from eq 18.

It is seen from Figure 8 that the data points for a-PMMA with small M_w in chloroform deviate upward slightly from those for the other polymer–solvent systems as $\tilde{z}$ is decreased for $\tilde{z} < 1$. The deviation may be regarded as arising from the solvent dependence of the bead friction, as mentioned above. The data points for PIB exhibit a similar tendency for $\tilde{z} \gtrsim 0.1$. As for this result, we must note that for PIB the relations $\langle S^2\rangle_0 = \langle S^2\rangle_\Theta$ and $C_\eta = 1$ have not been confirmed but only assumed.[2] Except for these few data points, all the data for the different polymer–solvent systems agree well with each other and form a single composite curve. It may be concluded from this finding that α_η is a function only of $\tilde{z}$, or, in other words, the quasi-two-parameter scheme is valid for α_η as well as for α_S, indicating that there is no draining effect in α_η at least for these systems.

It is seen that the solid curve is approximately consistent with the experimental results over the whole range of $\tilde{z}$ studied. This result is somewhat different from the previous one shown in Figure 6 of ref 2. The difference comes from the differences between the values of the HW model parameters determined from $\langle S^2\rangle_0$ and $[\eta]_\Theta$, which arise mainly from the difference between the observed and theoretical values of Φ_∞. The present results indicate that eq 18 may be of some practical use. However, we must note that it predicts the curvature somewhat different from that of the data points. In particular, the theoretical values are somewhat lower than the observed ones for $-0.5 \lesssim \log \tilde{z} \lesssim 0.5$ (or $0.3 \lesssim \tilde{z} \lesssim 3$), as found also in Figure 7.

Equation 18 predicts the value 0.8 for the exponent ν in the Houwink–Mark–Sakurada relation in the limit of large M. This may be considered to conflict with the fact that such a large value of ν has not been observed for flexible polymer solutions.[27] In fact, the slope of the solid curve at $\log \tilde{z} \simeq 1$ in Figure 8 is somewhat higher than that of the observed data; the theoretical value of ν is 0.79 for a-PMMA in chloroform at $M \simeq 10^6$, while its observed value is ca. 0.77. According to the theory, however, the asymptotic relation $\nu = 0.8$ is attained only at extremely large M ($\to\infty$). In the case of a-PS in benzene, ν is predicted to be only ca. 0.78 even at $M \simeq 10^7$. (Note that benzene is the best solvent for a-PS extensively studied so far.) Thus eq 18 cannot necessarily be rejected only from the point of view of the asymptotic exponent ν.

Concluding Remarks

In this work, we have investigated α_S and α_η as functions of z and also of $\tilde{z}$ for a-PMMA with $f_r = 0.79$ in acetone at 25.0 °C, in nitroethane at 30.0 °C, and in chloroform at 25.0 °C. It is found that the change in α_S with z depends on solvent, i.e., the excluded-volume strength, because of the effect of chain stiffness and that the effect remains large even for $M_w > 10^6$. However, α_S as a function of $\tilde{z}$ for a-PMMA is independent of solvent and coincides well with those for a-PS and PIB irrespective of the differences in chain stiffness and local chain conformation, yielding a single composite curve over the whole range of M_w studied. The YSS theory[4-6] is found to explain quantitatively the observed results.

The values of α_η for a-PMMA in the three good solvents have been calculated by taking account of the dependence of Φ_Θ (Φ_∞) on solvent, i.e., by dividing the cubed apparent viscosity-radius expansion factor $\bar{\alpha}_\eta^3$ determined in the conventional way by the constant factor C_η that explains the dependence of Φ_Θ on solvent. The behavior of α_η is found to be similar to that of α_S above; $\alpha_\eta(z)$ depends on solvent because of the effect of chain stiffness and $\alpha_\eta(\tilde{z})$ forms a single composite curve irrespective of polymer species and solvents. It is also found that the Barrett

equation[24] for α_η with $\tilde{z}$ in place of z may explain approximately the observed $\alpha_\eta(\tilde{z})$. Thus it may be concluded that both α_η and α_S are functions only of $\tilde{z}$, the quasi-two-parameter scheme being valid for them irrespective of the large differences in chain stiffness, local chain conformation, and solvent (the excluded-volume strength), indicating that there is no draining effect in α_η.

The unperturbed dimension $\langle S^2\rangle_0$ of a-PMMA is found to be independent of solvent in contradiction to the prevailing view.[20,21] Its dependence on solvent for a-PMMA has been exclusively discussed on the basis of its values determined from the Stockmayer–Fixman plot[28] of $[\eta]$. The present study shows that its dependence on solvent thus obtained from $[\eta]_\Theta$ for a-PMMA is only apparent and that the dependence on solvent of $[\eta]_\Theta$ must be regarded as arising from that of Φ_∞ (or Φ_Θ). As for the solvent dependence of Φ_∞ (or Φ_Θ) itself, a satisfactory theoretical explanation has not yet been presented.[16]

Acknowledgment. This research was supported in part by a Grant-in-Aid (02453100) from the Ministry of Education, Science, and Culture, Japan.

Appendix. Values of $\partial n/\partial c$ at 436 nm for a-PMMA in Acetone at 25.0 °C

sample	M_w	$\partial n/c$, cm^3/g
OM11	1.10×10^3	0.124_7
OM12	1.16×10^3	0.124_8
OM18	1.80×10^3	0.129_1
OM22	2.23×10^3	0.131_0
OM30	2.95×10^3	0.129_2
OM42	4.18×10^3	0.133_5
MM7	7.40×10^4	0.133_5

References and Notes

(1) Abe, F.; Einaga, Y.; Yoshizaki, T.; Yamakawa, H. *Macromolecules* **1993**, *26*, 1884.
(2) Abe, F.; Einaga, Y.; Yamakawa, H. *Macromolecules* **1993**, *26*, 1891.
(3) Horita, K.; Abe, F.; Einaga, Y.; Yamakawa, H. *Macromolecules* **1993**, *26*, 5067.
(4) Yamakawa, H.; Stockmayer, W. H. *J. Chem. Phys.* **1972**, *57*, 2843.
(5) Yamakawa, H.; Shimada, J. *J. Chem. Phys.* **1985**, *83*, 2607.
(6) Shimada, J.; Yamakawa, H. *J. Chem. Phys.* **1986**, *85*, 591.
(7) Yamakawa, H. *Annu. Rev. Phys. Chem.* **1984**, *35*, 23.
(8) Yamakawa, H. In *Molecular Conformation and Dynamics of Macromolecules in Condensed Systems*; Nagasawa, M., Ed.; Elsevier: Amsterdam, The Netherlands, 1988; p 21.
(9) Kratky, O.; Porod, G. *Recl. Trav. Chim. Pays-Bas* **1949**, *68*, 1106.
(10) Tamai, Y.; Konishi, T.; Einaga, Y.; Fujii, M.; Yamakawa, H. *Macromolecules* **1990**, *23*, 4067.
(11) Fujii, Y.; Tamai, Y.; Konishi, T.; Yamakawa, H. *Macromolecules* **1991**, *24*, 1608.
(12) Takaeda, Y.; Yoshizaki, T.; Yamakawa, H. *Macromolecules* **1993**, *26*, 3742.
(13) Yoshizaki, T.; Hayashi, H.; Yamakawa, H. *Macromolecules* **1993**, *26*, 4037.
(14) Dehara, K.; Yoshizaki, T.; Yamakawa, H. *Macromolecules* **1993**, *26*, 5137.
(15) Yamakawa, H.; Abe, F.; Einaga, Y. *Macromolecules* **1993**, *26*, 1898.
(16) Konishi, T.; Yoshizaki, T.; Yamakawa, H. *Macromolecules* **1991**, *24*, 5614.
(17) Einaga, Y.; Abe, F.; Yamakawa, H. *J. Phys. Chem.* **1992**, *96*, 3948.
(18) Berry, G. C. *J. Chem. Phys.* **1966**, *44*, 4550.
(19) Konishi, T.; Yoshizaki, T.; Saito, T.; Einaga, Y.; Yamakawa, H. *Macromolecules* **1990**, *23*, 290.
(20) Kurata, M.; Stockmayer, W. H. *Adv. Polym. Sci.* **1963**, *3*, 196.
(21) Quadrat, O.; Bohdanecký, M.; Mrkvičková, L. *Makromol. Chem.* **1981**, *182*, 445.
(22) Domb, C.; Barrett, A. J. *Polymer* **1976**, *17*, 179.
(23) Chen, Z. Y.; Noolandi, J. *J. Chem. Phys.* **1992**, *96*, 1540.
(24) Barrett, A. J. *Macromolecules* **1984**, *17*, 1566.
(25) Kirkwood, J. G.; Riseman, J. *J. Chem. Phys.* **1948**, *16*, 565.
(26) Shimada, J.; Yamakawa, H. *J. Polym. Sci., Polym. Phys. Ed.* **1978**, *16*, 1927.
(27) Fujita, H. *Macromolecules* **1988**, *21*, 179.
(28) Stockmayer, W. H.; Fixman, M. *J. Polym. Sci.* **1963**, *C1*, 137.